

Calculation of BCC Phase Diagram Using the Cluster-Site Approximation and First Principle Calculations

S. BOURKI and M. ZEREG

Theoretical Physics Laboratory, Department of Physics,
Faculty of Science University of Batna, Batna 05000 (Algeria)

E-mail: bourki_sabrina@univ-batna.dz

Abstract

A combination of First Principle Calculations (FPC) and statistical thermodynamics, *i.e.*, the Cluster-Site Approximation (CSA), is applied to describe the *bcc*-based Fe–Al phase diagram. The formation energies of ordered compounds are calculated using Full-Potential Linearised Augmented Plane Wave (FP-LAPW) results, and the entropy term is evaluated using the so-called modified Cluster Variation Method (CVM). The CSA model has been used to model the *bcc* bases in the Fe–Al system. The results obtained from this combination are compared with those obtained from the irregular tetrahedron approximation of the CVM, with the same FP-LAPW total energies.

INTRODUCTION

The Cluster Site Approximation (CSA) model was used to model *fcc* phases in several systems [1–3], this model is based on two approximations: Bragg–Williams [4, 5], and physically sounder Cluster Variation Method (CVM) [6, 7]. Since the clusters in the CSA are non-interfering (see Fig. 1, b), the independent variables are the site probabilities, thus retaining the advantage of the Bragg–Williams approxima-

tion, *i.e.*, the computation simplicity. And it can take into account both long and short range order, thus retaining the ability of CVM method [8]. This makes the CSA ideal for multicomponent phase diagram calculations [9].

The configurational entropy in the cluster-site approximation was derived for the *fcc* phases by Yang and Li [10, 11]; but the application of this method to the calculation of the *bcc* phase equilibria has never appeared in the literature. Then in the present study, formulations of the CSA for *bcc* structure were performed, based on the non-interfering irregular tetrahedron cluster in the CVM method.

Fe–Al is the most important binary system for both Al and Fe alloys, because it shows excellent corrosion and sulphidation resistance even at high temperature, reduced density compared to other ferrous alloys. Additional engineering advantages are low raw material and processing cost, all these advantages make the alloys of this system interesting engineering materials [14]. The set of phases used in the present work is formed by the A_2 -Al, A_2 -Fe, DO_3 -Fe₃Al, DO_3 -FeAl₃, B_2 -FeAl and B_{32} -FeAl compounds.

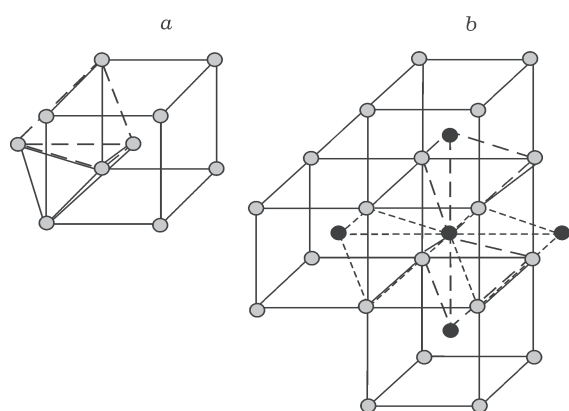


Fig. 1. Interfering (a) and non-interfering (b) irregular tetrahedrons in the *bcc* structure.

The basis set is kept limited here on purpose since only a simplified thermodynamic description of the bcc system based on the irregular tetrahedron approximation of the cluster site method is targeted.

The binary phase diagram Fe–Al was previously investigated experimentally [15], and theoretically using the combination between First Principle Calculations (FPC) and statistical model CVM [16]. With these new data of the FPC, the present work aims to investigate the ability of the CSA to describe the order-disorder transition in the bcc phases and show how the cluster-site approximation can be combined successfully with the First Principle Calculations.

CONVENTIONAL CVM

The cluster variation method is based on the concept of a basic cluster defined as a set of lattice points, chosen in such a way that it contains the maximum correlation length to be considered [17, 18]. In the present instance the irregular tetrahedron (IT) is considered to describe the superstructure of the cubic-centered structures [19]. It is the simplest tree dimensional cluster to take into account the first $\alpha\gamma$, $\alpha\delta$, $\beta\gamma$ and $\beta\delta$ and the second $\alpha\beta$, $\gamma\beta$ nearest pair interactions in the bcc lattice (see Fig. 1, a).

Defining the basic cluster we may write the corresponding thermodynamic functions. Firstly the internal energy for any bcc phase can be described as:

$$E = 6N \sum_{ijkl} \omega_{ijkl}^{\alpha\beta\gamma\delta} \rho_{ijkl}^{\alpha\beta\gamma\delta} \quad (1)$$

In this expression $\rho_{ijkl}^{\alpha\beta\gamma\delta}$ represents the probability of finding $\{\alpha\beta\gamma\delta\}$ IT cluster with configuration $\{ijkl\}$, and $\omega_{ijkl}^{\alpha\beta\gamma\delta}$ are the eigenenergy associated with this configuration

$$\omega_{ijkl}^{\alpha\beta\gamma\delta} = \frac{1}{4}(\omega_{ij}^2 + \omega_{kl}^2) + \frac{1}{6}(\omega_{ik}^1 + \omega_{il}^1 + \omega_{jk}^1 + \omega_{jl}^1) \quad (2)$$

where $\omega^{(1)}$ and $\omega^{(2)}$ presents respectively the nearest and next nearest-neighbour pair interactions.

The derivation of the CVM entropy formula was thoroughly outlined in several reviews [20] and shall not be discussed here. In the bcc lattice, the configurational entropy is written as:

$$S/K_B = \log \left(\frac{\left\{ \prod_{ijk} (Nz_{ijk})! \right\}^{12} \left\{ \prod_i (Nx_i)! \right\}}{\left\{ \prod_{ijkl} (N\rho_{ijkl}^{\alpha\beta\gamma\delta})! \right\}^6 \left\{ \prod_{ik} (Ny_{ik}^{(1)})! \right\}^4 \left\{ \prod_{ij} (Ny_{ij}^{(2)})! \right\}^3} \right)$$

where x_i , y_{ik}^1 , y_{ij}^2 , z_{ijk} and $\rho_{ijkl}^{\alpha\beta\gamma\delta}$ are the cluster probabilities of finding the atomic configurations specified by the subscript at a point, nearest-neighbor pair, second nearest-neighbor pair, at a triangle and at a tetrahedron cluster, respectively. N presents the number of lattice points.

To obtain the phase equilibrium conditions in this method, the grand potential function is used:

$$\Omega(T, \mu_1^*, \mu_2^*) = E - TS_{\text{conf}} - \sum_{i=1}^2 \mu_i^* x_i + \lambda \left(1 - \sum_{ijkl} \rho_{ijkl} \right) \quad (4)$$

where x_i is the mole fraction of component i , λ is the Lagrange multiplier to the constraint

$\sum_{ijkl} \rho_{ijkl} = 1$, and μ^* called the effective chemical potential is defined as $\mu_A^* = (\mu_A - \mu_B)/2$ where μ_i is the absolute chemical potential of element i .

The equilibrium values of the grand potential Ω and corresponding configurations of clusters are obtained by minimizing this function with respect to $\rho_{ijkl}^{\alpha\beta\gamma\delta}$:

$$\left. \frac{\partial \Omega}{\partial \rho_{ijkl}^{\alpha\beta\gamma\delta}} \right|_{T, \mu^*} = 0 \quad (5)$$

MODIFIED CVM

In spite of its successes, a major disadvantage of the CVM is the large number of independent variables in the free energy functional when it is applied to multicomponent solutions [8]; *i.e.*, if an alloy contains N components, the

number of independent variables is N^n , where n is the number of atoms in the cluster chosen. But in the CSA method it is in the order of $N \times n$, because the independent variables are the site probabilities x_i^q , $q = \alpha, \beta, \gamma, \delta$, instead of the cluster probabilities $\rho_{ijkl}^{\alpha\beta\gamma\delta}$ in the CVM approximation.

The basic idea of the CSA method is to define the CVM free energy with non-interfering clusters: they are permitted only to share corners; therefore sub-cluster energies do not enter into the energy equation, *i.e.* as a correction term. This method was used to calculate different *fcc*-based phase diagrams with great success [1–3, 9], but not for the *bcc*-based alloys.

In this paper we focus our attention on the *bcc* alloys, and since the CSA is based on the cluster variation method, the main objective is to define the free energy of the system with non-interfering clusters, *i.e.*, the so-called modified CVM (see Fig. 1, b). Using the generalization proposed by C. Colinet [21], the internal energy for a system of N site is:

$$E = \gamma N \sum_{ijkl} \omega_{ijkl}^{\alpha\beta\gamma\delta} \rho_{ijkl}^{\alpha\beta\gamma\delta} \quad (6)$$

where γ is the number of non-interfering clusters per site, and the tetrahedron energies will be rewritten as:

$$\omega_{ijkl}^{\alpha\beta\gamma\delta} = \omega_{ij}^2 + \omega_{kl}^2 + \omega_{ik}^1 + \omega_{il}^1 + \omega_{jk}^1 + \omega_{jl}^1 \quad (7)$$

non-interfering clusters always result in two term for the entropy, as:

$$S / K_B = \ln \left(\frac{\left\{ \prod_i (N x_i) \right\}^{(n\gamma - 1)}}{\left\{ \prod_{ijkl} (N \rho_{ijkl}^{\alpha\beta\gamma\delta}) \right\}^\gamma} \right) \quad (8)$$

Of course, this method decreases the computational time, because we can see in Eq. (8) that the number of dependent variables decreases, *i.e.* the pair and triangle probabilities $y_{ij}^{(1)}$, $y_{ij}^{(2)}$ and t_{ijk} do not appear in the entropy term, but the number of independent parameters is still N^n . However, it gives a good starting point for generalized cluster site approximation to all alloy structures.

CLUSTER-SITE APPROXIMATION

The cluster-site approximation is an adaptation of the generalized quasi-chemical method, introduced many years ago by Fowler for treating atom-molecule equilibria in gases, and used for clusters in solid solutions by Yang and Li [10, 11].

The free energy in the CSA approximation takes the same form as that in the modified CVM in the above section, internal energy (E) is given by Eq. (6) and Eq. (7) and the configurational entropy (S_{cont}) by Eq. (8). Therefore we can rewrite the molar free energy as:

$$F_m = \gamma RT \left(\sum_{i=1}^4 P_A^i x_A^i - \ln \phi \right) - (4\gamma - 1) RT \sum_q \sum_i f_i x_i^q \ln x_i^q \quad (9)$$

here ϕ is the cluster partition function related to the cluster energies ω_{ijkl} mentioned above by:

$$\phi = \sum_{ijkl}^{2^n} \exp \left[\left(\sum_{i=1}^4 P_n^i \right)_{ijkl} - \omega_{ijkl} \right] \quad (10)$$

In Eqs. (9) and (10) the x_i^q values are the sub-lattice species concentrations, and the P_A^i values, are new parameters related to the species chemical potentials. Since they are related to the x_i^q values, only one of them is required as independent variables.

The first step in the search for equilibrium between two phases is to minimize the grand potential (Ω), with respect to the site probabilities under the constraints of constant temperature, and effective chemical potential (μ^*). The minimization process was performed by the Natural Iterative (NI) algorithm, developed by Kikuchi [22], and the equilibrium parameters P_i^q values in each sub-lattice $q = \alpha, \beta, \gamma, \delta$ can be done as:

$$P_i^q = \left(\frac{x_i^q}{x_B^q} \right)^{\gamma - 0.25} \exp \left(\frac{\mu_i^* - \mu_B^*}{4\gamma RT} \right) \quad (11)$$

if the site is occupied by the species B ($i = B$), these parameters are equal to unity, *i.e.*

$$P_B^q = 1, \quad q = \alpha, \beta, \gamma, \delta \quad (12)$$

and the cluster probabilities can be calculated explicitly as follows:

$$P_{ijkl} = \frac{P_i^\alpha P_j^\beta P_k^\gamma P_l^\delta}{\varphi} \exp(-\omega_{ijkl} / RT) \quad (13)$$

The number of independent variables decreases to four instead of 16 in the tetrahedron-CVM approximation, that makes the CSA very promising for the multicomponent phase diagram calculations.

Among various techniques of the first principle investigation, it is recognized that the combination of the electronic structure total energy calculation with statistical mechanics calculations by the CVM [23–26] provides a reliable tool.

In the present study, we adopted FP-LAPW electronic structure calculations to obtain the total energies of a set of selected ordered compound. These data are plugged into the CSA in order to obtain phase boundaries in a *bcc* alloys system.

RESULTS FOR THE Fe–Al SYSTEM

Table 1 shows the total energies of the six compounds forming the basis for the cluster-site approximation applied to the Fe–Al system, and Table 2 presents the formation energies of the *bcc* compounds, as well as the corresponding equilibrium lattice constant. The analysis of the formation energies shows that the most stable *bcc*-based compound in this basis set is B_2 .

In the Fe–Al system there are different structural phases, since the objective of this study was to explore the application of the CSA

TABLE 1
Fe–Al cohesive energies of the *bcc* phases obtained by FP-LAPW [16]

Alloy	Space group	Structure	E_c , eV/at.
Fe	$Im\bar{3}m$	A_2	-6.696
Fe_3Al	$Fm\bar{3}m$	DO_3	-6.127
FeAl	$Fd\bar{3}m$	B_{32}	-5.353
FeAl	$Pm\bar{3}m$	B_2	-5.474
$FeAl_3$	$Fm\bar{3}m$	DO_3	-4.378
Al	$Im\bar{3}m$	A_2	-3.477

TABLE 2

The formation energies and equilibrium lattice parameters of the various phases in the Fe–Al system

Alloy	E_f , J/mol	a , Å
Fe	0	2.801
Fe_3Al (DO_3)	-21273.23	2.914
FeAl (B_{32})	-24911.12	2.933
FeAl (B_2)	-36282.55	2.910
$FeAl_3$ (DO_3)	-9275.42	3.042
Al	0	3.257

to the *bcc* structure, only the *bcc* phases were modeled. Thus the phases that will be studied in this paper are two disordered phases (A_2), and four ordered phases with DO_3 , B_{32} and B_2 superstructure.

Figure 2 shows the formation energies as a function of composition for all the compounds of this binary system, calculated from the FP-LAPW results [16]. From this Figure we can expect by plotting the ground state line the appearance of the B_2 -FeAl and the DO_3 - Fe_3Al superstructure in the phase diagram at low temperature, and the B_{32} -FeAl end DO_3 - $FeAl_3$ will always be metastable and will not appear in the equilibrium phase diagram.

The Fe–Al phase diagram shown in Fig. 3 is calculated using the cluster site approximation, and it illustrates the ability of the present modeling to describe the *bcc* phases.

The CSA in conjunction with First principle calculations is capable of fitting the order-disorder equilibrium, the phase diagram calculat-

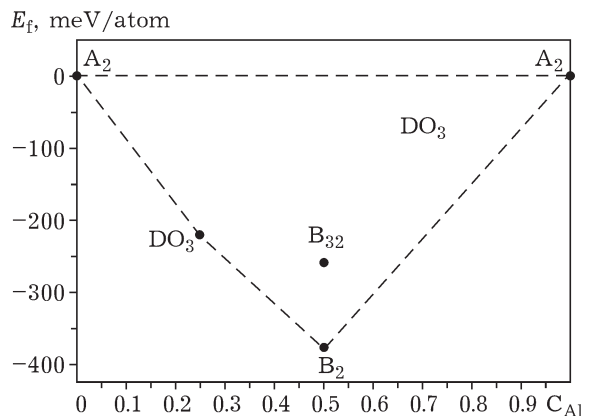


Fig. 2. Formation energies as a function of composition for all the compounds studied.

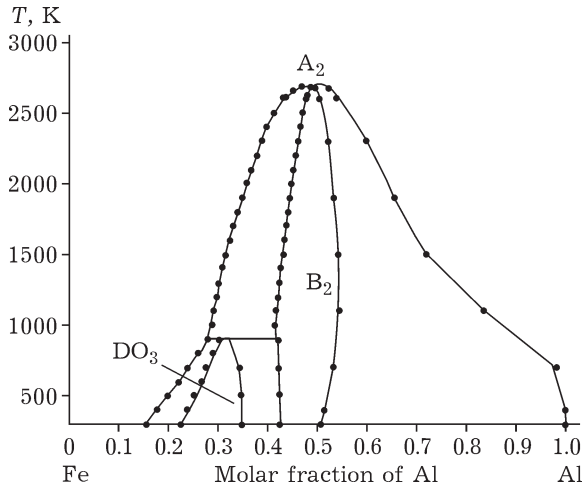


Fig. 3. Fe-Al phase diagram calculated using the CSA model for $\gamma = 1.5$.

ed indicates that the B_2 -FeAl phase is stable over an extended composition range up to the order-disorder transition temperature of 2650 K and the DO_3 -Fe₃Al compound, by contrast is found to be stable up to 950 K, where it undergoes a peritectoid reaction to $B_2 + A_2$; these results indicated that the previous predictions of the phases that will be appearing in the phase diagram from the formation energies are correct.

The transition temperature obtained experimentally is 1583 K [15]. Hence, the present results of 2650 K are overestimated by 1067 K. The overestimation originates from the reason that our calculations are based on a rigid lattice model, which neglects important contributions to the alloy free energy, like the vibrational term.

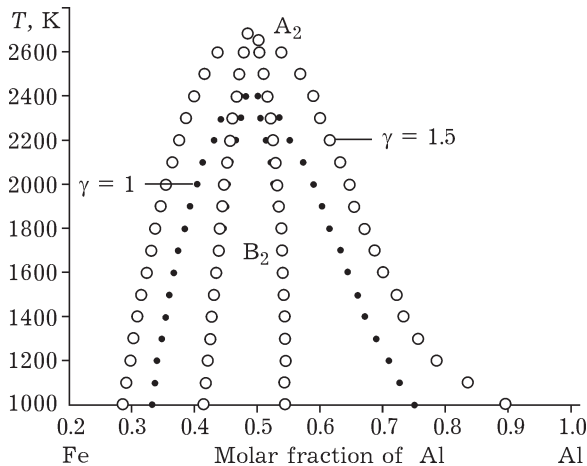


Fig. 4. Calculated order-disorder transition $A_2 \rightarrow B_2$ for $\gamma = 1.5$.

Kikuchi and Jindo [27] demonstrated that the temperature scale of prototype phase diagrams can be reduced to about 40 % of the rigid lattice model value by explicitly taking into account the positional degree of freedom of the atoms with the continuous displacement cluster variation method.

It is worth pointing out that Ormeno *et al.* [14] calculated the phase diagram of the Fe-Al system using the first principle method without spin polarization (Fig. 4, a) and with spin polarization (see Fig. 4, b). The calculated phase diagrams are topologically similar to that shown in Fig. 3. The transition temperature between B_2 and A_2 states is considerably higher in this calculation than that calculated in the present work.

Figure 5 shows the order-disorder transition ($B_2 \rightarrow A_2$) calculated using $\gamma = 1$ and $\gamma = 1.5$, respectively. An important characteristic of these calculations is the relationship between the adjustable parameter γ and the critical temperature T_c

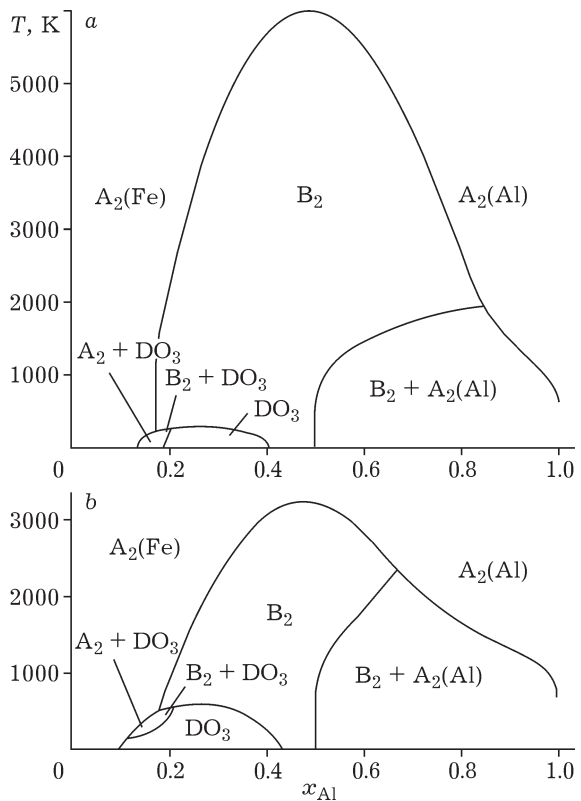


Fig. 5. Phase diagram of bcc Fe-Al alloys as obtained from *ab initio* calculation [14]: a - without spin polarization, b - with spin polarization.

of the order-disorder transition, which makes the determination of γ value more accurate.

CONCLUSIONS

In the present study, a general formula of the CSA for the bcc structure was derived, based on the entropy expressions reported in other works, and the so-called modified CVM. The model was applied to the bcc phases in the Fe–Al system where the energetic term was determined using the FPC results.

In general, the obtained results are quite encouraging because all the predicted phases appear in the calculated phase diagram. In addition, they are in good agreement with the previously calculated Fe–Al system using the *ab initio* method.

Even though not as physically sound as the CVM, the cluster site approximation has the considerable advantage of computational simplicity over the CVM and seems very promising for the calculation of phase diagrams in multicomponent systems.

REFERENCES

- 1 W. A. Oates, F. Zhang, S. L. Chen, Y. A. Chang, *Phys. Rev. B*, 59, 17 (1999) 11221.
- 2 F. Zhang, Y.A. Chang, Y. Du *et al.*, *Acta. Mater.*, 51 (2003) 207.
- 3 W. Cao, Y. A. Chang, J. Zhu *et al.*, *Ibid.*, 53 (2005) 331.
- 4 W. L. Bragg, E. J. Williams, *Proc. Roy. Soc.*, A145 (1934) 699.
- 5 W. L. Bragg, E. J. Williams, *Ibid.*, A151 (1935) 540.
- 6 R. Kikuchi, *Phys. Rev.*, 81 (1951) 988.
- 7 R. Kikuchi, *Acta Metallurgica*, V 25 (1977) 195.
- 8 Y. A. Chang, S. Chen *et al.*, *Progr. Mat. Sci.*, 49 (2004) 313.
- 9 W. Cao, J. Zhu, Y. Yang *et al.*, *Acta. Mater.*, 53 (2005) 4189.
- 10 C. N. Yang, *J. Chem. J. Phys.*, 13 (1945) 66.
- 11 C. N. Yang, Y. Li, *Ibid.*, 7 (1947) 59.
- 12 L. G. Ferreira, A. A. Mbaye, A. Zunger, *Phys. Rev.*, B35 (1987) 6475.
- 13 F. Zhang, W. A. Oates, S. L. Chen, Y. A. Chang, *Intermetallics*, 9 (2001) 5.
- 14 P. G. G. Ormeno and H. M. Petrilli, *Calphad*, 26, 4 (2002) 573.
- 15 M. Hansen, *Constitution of Binary Alloys*, McGraw-Hill Book Co., New York, 1958.
- 16 P. G. G. Ormeno, Determination of the Fe–Al Phase Diagram Using the First Principle Calculation, PhD thesis, Sao Paulo University, 2002, Brazil.
- 17 R. Kikuchi, J. M. Sanchez *et al.*, *Acta Metallurgica*, 28 (1980) 651.
- 18 J. M. Sanchez and D. de Fontaine, *Phys. Rev. B*, 17 (1978) 2926.
- 19 R. Kikuchi and G. M. Van Baal, *Scripta Metallurgica*, 8 (1974) 425.
- 20 J. M. Sanchez and D. de Fontaine, *Phys. Rev. B*, 17 (7) (1978) 2926.
- 21 C. Colinet, *Thec. Ingen.*, AF4 061 (1998) 1.
- 22 R. Kikuchi, *Prog. Theor. Phys. Suppl.*, 115(1994).
- 23 A. Pasturel, C. Colinet *et al.*, *J. Phys. Condens. Matter*, 4 (1992) 945.
- 24 M. Sluiter and D. de Fontaine, *Phys. Rev. B*, 42 (16) (1990) 10460.
- 25 T. Mohri and Y. Chen, *J. All. Comp.*, 383 (2004) 23.
- 26 P. G. G. Ormeno, H. M. Petrilli and C. G. Schön, *Scripta Mater.*, 53 (2005) 751.
- 27 R. Kikuchi, K. M. Jindo, *Calphad*, V26 (2002) 33.